Journal of Photochemistry and Photobiology A: Chemistry 224 (2011) 102–109

Contents lists available at SciVerse ScienceDirect

Journal of Photochemistry and Photobiology A: Chemistry

journal homepage: www.elsevier.com/locate/jphotochem

Influence of pH on dendritic structure of strongly fluorescent persulfate-treated poly(amidoamine) dendrimer

Govindachetty Saravanan*, Hideki Abe**

Advanced Electronic Materials Center, National Institute for Materials Science, 1-2-1 Sengen, Tsukuba, Ibaraki 305-0047, Japan

ARTICLE INFO

Article history:
Received 9 March 2011
Received in revised form 25 August 2011
Accepted 9 September 2011
Available online 16 September 2011

Keywords:
Poly(amidoamine) dendrimer
Ammonium persulfate treatment
Fluorescence
Dendritic structure
FT-IR spectroscopy
X-ray photoelectron spectroscopy

ABSTRACT

The influence of pH on the dendritic structure of strongly fluorescent ammonium persulfate (APS)-treated poly(amidoamine) (PAMAM) dendrimers was examined. The APS-treated PAMAM dendrimers were prepared by aging of 0.2 mM aqueous solutions of a hydroxyl groups-terminated, generation-five PAMAM (G5OH) dendrimer together with 200 μl of 0.1 M APS solutions. The G5OH dendrimer showed an absorbance at 280 nm, which was red-shifted to 360 nm after APS treatment. The APS-treated G5OH dendrimer solutions emitted much stronger fluorescence than the pristine G5OH dendrimer solutions when irradiated at 360 nm. The pH of the G5OH dendrimer solution is 7.6 while that of the APS-treated G5OH dendrimer solution is 5.2. The pore surface of both pristine and fluorescent G5OH dendrimers was altered more significantly under acidic than basic conditions. The tertiary amine groups of the pore surface of the fluorescent G5OH dendrimers were protonated by APS treatment as well as under the acidic condition; therefore, the pore surface of the G5OH dendrimer was filled with tertiary ammonium cations, which were, however, further deprotonated under basic conditions. The sulfur anions (VI and II) were generated during the hydrolysis of APS, which were interacted with the G5OH dendrimers under both acidic and basic conditions.

1. Introduction

It has been found that bio-compatible, nonimmunogenic, poly(amidoamine) (PAMAM) dendrimers emit purely intrinsic but weak blue-fluorescence upon irradiation of UV light [1]. Despite the potential versatility of PAMAM dendrimers, weakness in the fluorescence has limited their applications in the biomedical area. Therefore, research on the enhancement of the fluorescence of PAMAM dendrimers has been fueled by their potential utilization in practical biomedical applications, such as specific targeting, imaging, and/or treatments of cancer [2].

Strong, monochromatic fluorescent PAMAM dendrimers have been achieved by labeling of fluorescent ligands (e.g., fluorescein isothiocyanate-folic acid) [3] and imaging dyes (e.g., rhodamine and carboxyfluorescein) [4] on the peripheral functional groups of PAMAM dendrimers as well as the synthesis of metal nanoparticles and/or quantum dots on the pore surface of the PAMAM dendrimer (PAMAM dendrimer-encapsulated nanoparticles, PAMAM DENs) [5–7]. The encapsulated metal nanoparticles and/or quantum dot PAMAM DENs showed strong enough florescence emission upon irradiation of UV light. However, PAMAM dendrimers played the role of an optically inert support that dispersed the nanoparticles and/or nanodots in solvents. Fabrications on both the peripheral groups and the pore surface of PAMAM dendrimers by novel fluorophores without altering the physical and chemical properties are often complicated due to the requirements of toxic compounds and multiple synthetic steps. Therefore, purely intrinsic, strong fluorescence emissions of PAMAM dendrimers have been anticipated for biomedical applications.

Lee et al. showed strong, monochromatic fluorescence of generation-two, hydroxyl-terminated PAMAM dendrimers (G2OH) (quantum yield 58 ± 5% relative to quinine sulfate) in the absence of fluorophores on the pore surface or peripheral functional groups [8]. G2OH dendrimers showed enhanced fluorescence when treated under oxidizing conditions (persulfate-treated PAMAM dendrimers) for several hours. Fluorescent persulfate-treated PAMAM dendrimers have been prepared by aging of PAMAM dendrimers together with persulfate solutions. It has been reported that the pH of persulfate solutions falls to the acidic condition due to the generation of permonosulfuric acid during the aging processes [9]. Although the strong fluorescence behavior of persulfate-treated PAMAM dendrimers has been examined, little information has been obtained about the dendritic structures of persulfate-treated PAMAM dendrimers at different pH.

Various studies about PAMAM dendrimers comprising different generation and peripheral functional groups indicate that

* Corresponding author. Tel.: +81 29 851 3354; fax: +81 29 859 2801.
** Corresponding author.
E-mail addresses: saravanan.govindachetty@nims.go.jp (G. Saravanan), abe.hideki@nims.go.jp (H. Abe).

1010-6030/$ – see front matter © 2011 Elsevier B.V. All rights reserved.
doi:10.1016/j.jphotochem.2011.09.012

the fluorescence behavior of PAMAM dendrimers are significantly influenced by the dendritic structures or the pore surface of the functional groups of PAMAM dendrimers rather than the peripheral functional groups [10]. The amide carbonyls and N–H moieties of dendrimers interact on the pore surface through both inter- and intramolecular hydrogen bonding in aqueous solutions [11]. Furthermore, the strength of hydrogen bonding in the dendrimer is enhanced under acidic conditions [12]. The higher generation of PAMAM dendrimers emits considerable fluorescence and is comparable with the lower generation [13]. PAMAM dendrimers emit strong fluorescence at lower pH, and the tertiary amine groups of PAMAM dendrimers are protonated, filling the whole dendritic interior with cations in an acidic medium [12,13a,13b]. By considering the falling of pH of persulfate solutions during hydrolysis, detailed structural characterizations of persulfate-treated PAMAM dendrimers at different pH and the influence of pH on the dendritic structures of PAMAM dendrimers will be needed to understand the strong fluorescence behavior of persulfate-treated PAMAM dendrimers.

In this work, the dendritic structures of ammonium persulfate-treated PAMAM dendrimers (generation-five, hydroxyl-terminated) (hereafter called APS-G5OH) were examined at different pH. The optical properties of APS-G5OH were examined by UV–visible and fluorescence spectroscopy. Fourier-transform IR (FT-IR) and X-ray photoelectron spectroscopy (XPS) techniques were employed to examine the influence of pH on the dendritic structures of PAMAM dendrimers. Pristine generation-five, hydroxyl-terminated PAMAM dendrimers (hereafter called G5OH) were utilized as a reference to compare the optical properties and dendritic structure of APS-G5OH at different pH.

2. Experimental

2.1. Materials

A 5 wt.% methanol solution of G5OH was purchased from Aldrich. Ammonium persulfate ($(NH_4)_2S_2O_8$) (APS) was purchased from Kishida Chemicals. Hydrochloric acid and sodium hydroxide were purchased from Kishida Chemicals. All chemicals were used as received for sample preparation without any further purification. Purified water was prepared using the Millipore system.

Aqueous solutions of 0.2 mM G5OH dendrimers and 0.1 M APS were prepared and stored in the refrigerator. 5 ml of 0.2 mM G5OH solutions was stirred in the presence of 0.2 ml of 0.1 M APS for several days at room temperature. Similarly, 5 ml of 0.2 mM G5OH solutions was prepared for reference purposes but in the absence of APS. The APS-G5OH solution turned to pale yellow, while the pristine G5OH solution remained colorless after 8 days. Diluted hydrochloric acid and sodium hydroxide were used to adjust the pH.

2.2. Characterization

UV–visible and fluorescence spectra of pristine G5OH and APS-G5OH solutions were collected on a Hitachi U-2900 and F-7000, respectively. A Xenon lamp, operated at 150 W, was utilized as an excitation source. The sample solutions were irradiated at 360 nm for the emission spectra and 450 nm for the excitation spectra. FT-IR spectra were obtained in a single-beam absorbance mode at a resolution of 4 cm^{-1} with a Perkin-Elmer FT-IR (Spectrum GX-R) system equipped with a MIRTGS detector. FT-IR samples were prepared by dropping 200 μl of sample solutions onto the surface of CaF_2 crystals and drying them under a vacuum. X-ray photoelectron spectroscopy (XPS) with a Thermo Scientific Theta probe of PAMAM dendrimer films on carbon substrates was performed using an Al Kα monochromatized X-ray beam at a constant dwell time of 50 ms. An aliquot of 100 μl of sample solutions was dried onto carbon substrates under a vacuum. Carbon black (Vulcan XC-72, Cabot Co., Ltd.) was mixed with the sample solutions for XPS measurements to avoid the charging effect. X-ray scans were performed with a 400 μm^2 sampling area using pass energies of 200 eV for a wide scan and of 100 eV for a narrow scan. The anode voltage and current were 14 kV and 7.2 mA, respectively. All core-level spectra were obtained at photoelectron takeoff angles between 20.31° and 79.69° with respect to the PAMAM dendrimer films.

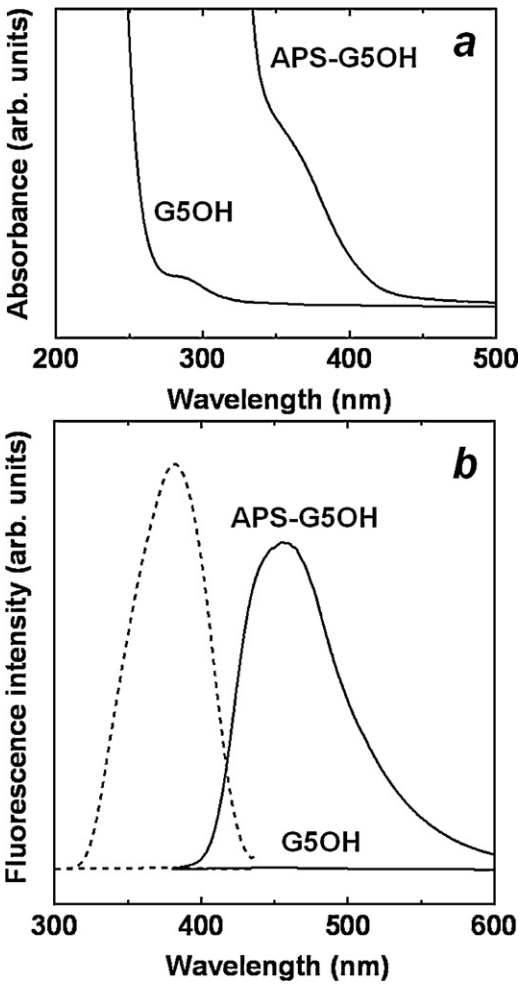

Fig. 1. UV–visible spectra (a) and emission (solid line) and excitation (dashed line) spectra (b) for an aqueous solution of 0.2 mM G5OH and APS-G5OH.

3. Results and discussion

3.1. Optical properties of pristine and APS-G5OH dendrimer

Fig. 1a shows the UV–visible spectra for an aqueous solution of 0.2 mM G5OH and APS-G5OH. G5OH showed a weak shoulder peak at 280 nm, may be assigned to the n–π* transition of the branching units of dendrimer molecules [1d]. APS-G5OH also showed a weak shoulder peak; however, the peak shifted substantially to a higher wavelength and was observed at around 360 nm. The aging of the PAMAM dendrimer in the presence of a persulfate solution resulted in a larger red shift in wavelength. Fig. 1b shows the emission and excitation spectra for an aqueous solution of 0.2 mM G5OH and APS-G5OH. The G5OH dendrimer showed weak emission and excitation bands at 445 and 370 nm, respectively. However, APS-G5OH showed very strong emission and excitation bands which

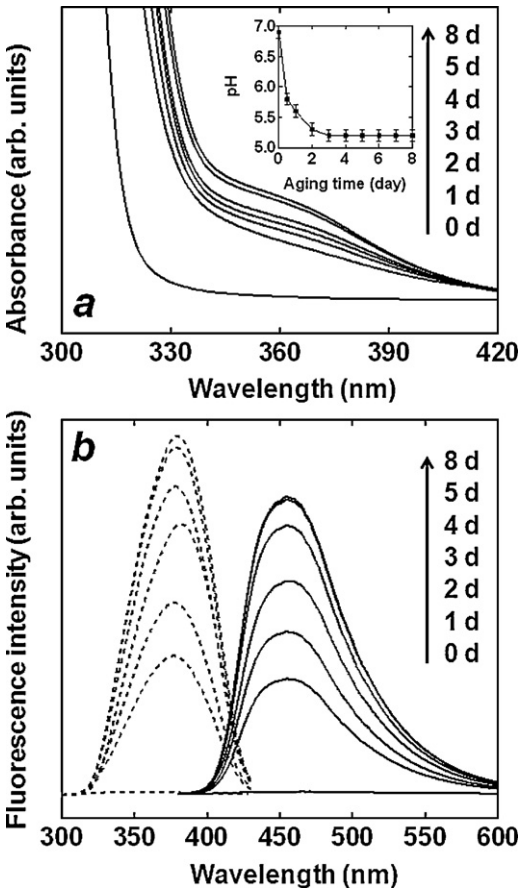

Fig. 2. UV–visible spectra (a) and emission and excitation spectra (b) for an aqueous solution of 0.2 mM G5OH in the presence of APS at different aging interval. Inset shows the pH dependences as a function of aging interval.

were shifted to a higher wavelength ca. 10 nm, consistently with other reported results [8].

The aging effects of G5OH in the presence of APS were also examined. Fig. 2a shows the successive UV–visible spectra for an aqueous solution of 0.2 mM APS-G5OH at various aging interval. The weak shoulder peak of G5OH showed red shift in wavelength with increasing aging. The intensity of emission and excitation bands for APS-G5OH became much stronger with increasing aging as shown in Fig. 2b, indicating that the optical properties of G5OH were altered significantly during aging. It should be noted that pH of APS-G5OH solution decreased with increasing aging interval and reached a constant pH value after 2 days as shown in the inset of Fig. 2a. pH of the pristine G5OH solution is 7.6, while pH of the APS-G5OH is 5.2. This is because permonosulfuric acid, sulfuric acid, peroxymonosulfate, and hydrogen peroxide were generated during the hydrolysis of APS by the following reactions [9].

$$(NH_4)_2S_2O_8 + H_2O \rightarrow H_2SO_5 + (NH_4)_2SO_4$$

$$H_2SO_5 + H_2O \rightarrow H_2SO_4 + H_2O_2$$

$$S_2O_8{}^{2-} + 2H_3O^+ \rightarrow 2HSO_4{}^- + H_2O_2$$

$$H_2O_2 \rightarrow H_2O + 1/2O_2$$

The red shift in absorption band as well as the enhancement in the fluorescence of APS-G5OH is most likely attributed to changes in the dendritic structure due to the falling of pH. Wang et al. reported that generation-four amine-terminated PAMAM dendrimers emitted strong fluorescence under acidic conditions and also showed

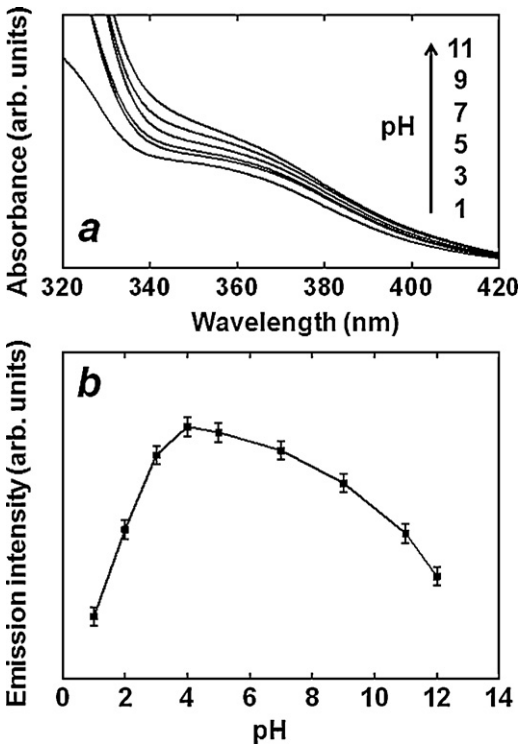

Fig. 3. UV–visible spectra (a) and emission intensities (b) for an aqueous solution of aged 0.2 mM APS-G5OH at different pH.

that the fluorescence emission of PAMAM dendrimers is strongly dependent on the pH of the sample solution [10].

The optical properties of APS-G5OH were further examined at different pH. Fig. 3a shows the UV–visible spectra for an aqueous solution of 0.2 mM APS-G5OH at different pH. The weak shoulder peak of APS-G5OH showed red shift in wavelength with increasing pH. Fig. 3b shows the emission intensities of an aqueous solution of APS-G5OH at different pH. The emission intensity of APS-G5OH showed a critical pH at 4, where the strong fluorescence emission was observed. However, the emission intensity of APS-G5OH decreased rapidly both under acidic condition at less than 4 and basic condition. The similar critical pH has also been observed in the case of generation 2 and 4, amine terminated PAMAM dendrimer [10]. These results indicate that dendritic structure of APS-G5OH was altered significantly by changing of pH.

3.2. FT-IR spectra of pristine and APS-G5OH dendrimers

FT-IR spectroscopic measurements were performed over pristine G5OH and fluorescent APS-G5OH to examine the dendritic structures after APS treatment. Fig. 4 shows the FT-IR spectra of G5OH and APS-G5OH films that were prepared from the as-prepared sample solutions on the CaF_2 substrate. The G5OH film showed a shoulder and a characteristic band at approximately 3500 and 3300 cm^{-1} for O–H (terminal groups) and a hydrogen-bonded N–H stretching band of the amide functional groups of the PAMAM dendrimer, respectively [11b]. The band was observed at 3090 cm^{-1} and can be assigned to the overtone of the (N–H) bending/(C–N) stretching modes. Symmetric and asymmetric stretching vibrations of methylene groups were observed at 2837 and 2942 cm^{-1}, respectively (Fig. 4a) [11b]. The shoulder band for the surface hydroxyl group remained at approximately the same position in the case of the APS-G5OH film. However, a broad band was observed in the region ~3300 cm^{-1} for the APS-G5OH dendrimer due to the overlapping of hydrogen-bonded N–H

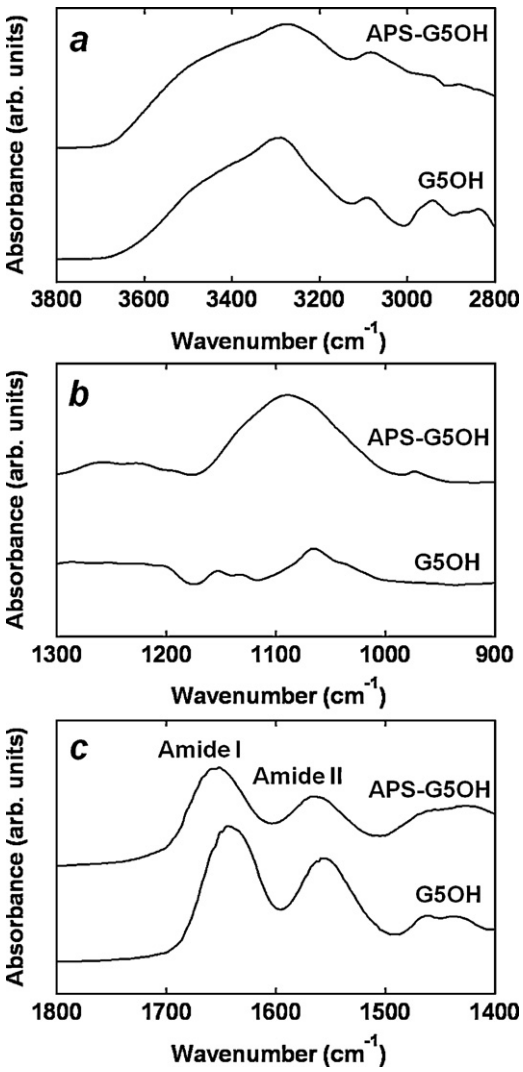

Fig. 4. FT-IR spectral profiles of as-prepared G5OH and APS-G5OH films.

of the amide functional group and anti-symmetric stretching vibrations of ammonium ions, which can also be observed in the same region [14]. Moreover, the symmetric and asymmetric stretching vibrations of methylene groups of G5OH became weaker after APS treatment. Fig. 4b shows a C–N stretching band for tertiary amines of G5OH, which was observed at 1066 cm^{-1} [15]. In addition to that, a weak doublet peak was observed in the region of 1132–1153 cm^{-1} for skeletal C–C stretching [11b]. However, the APS-G5OH showed a broad band in the region of 1175–990 cm^{-1} due to the overlapping of the C–N stretching band, skeletal C–C stretching band, asymmetric stretching band of SO_4^{2-} (1090 cm^{-1}), and HO–S–OH symmetric bending (1137 cm^{-1}) (see text for details) [11b,16]. In addition, a weak band at 972 cm^{-1} also evidenced the existence of SO_4^{2-} in APS-G5OH [14b]. G5OH showed two strong absorption peaks at 1642 and 1555 cm^{-1} that can be assigned to a carbonyl (C=O) stretching mode of the amide group (amide I) and (N–H) bending/(C–N) stretching modes (amide II), respectively as shown in Fig. 4c [11b,17]. In addition to these peaks, a couple of weak peaks for CH_2 scissoring modes were observed in the region from 1435 to 1460 cm^{-1} [18]. Both the amide I and II stretching bands of APS-G5OH shifted to a higher wavenumber by 10 cm^{-1} relative to that for pristine G5OH. These results indicate that the dendritic structure or the pore surface of the APS-G5OH is significantly altered by APS treatment and, thus, the dendritic structure of APS-G5OH is different from that of pristine G5OH.

3.2.1. FT-IR spectra of pristine and APS-G5OH dendrimer under different pH

The pristine G5OH and APS-G5OH films were examined further at different pH to ensure the influence of pH on the dendritic structure. Fig. 5 shows the FT-IR spectra for G5OH and APS-G5OH films that were prepared from the as-prepared PAMAM dendrimer solutions at different pH. At any pH, the stretching bands of surface hydroxyl groups (≈3490 cm^{-1}) of G5OH did not change. The band for the hydrogen-bonded N–H of the amide functional group of G5OH became broader under acidic conditions, likely due to the enhancement in the strength of hydrogen bonding with near-pore-surface functional groups as well as the protonation of tertiary amine groups [12,13]. However, at higher pH, the hydrogen-bonded N–H stretching band could be clearly seen. The stretching bands for the overtone of amide II and symmetric and asymmetric stretching modes of methylene groups did not change at any pH (Fig. 5a). Fig. 5b shows the FT-IR spectra for APS-G5OH films at different pH. At any pH, no significant changes were observed for the stretching bands of either the surface hydroxyl- or hydrogen-bonded N–H groups; however, the N-H stretching band was slightly broader at higher pH. The C–N stretching band of tertiary aliphatic amines of as-prepared G5OH did not change at any pH. Skeletal C–C stretching bands could be clearly seen when the pH was above 3 (Fig. 5c). However, a broad band was observed in the region of 1170–990 cm^{-1} for APS-G5OH under acidic conditions. This broad band was separated into multiple bands when the pH of the solutions is above 7 that can be assigned for C–N stretching band and skeletal C–C stretching, asymmetric stretching band of SO_4^{2-} (1090 cm^{-1}) and HO–S–OH symmetric bending (1137 cm^{-1}) [11b,16]. The asymmetric stretching band of SO_4^{2-} and HO–S–OH symmetric bending can be clearly seen under basic conditions and is stronger at higher pH (Fig. 5d). Fig. 5e and f shows the characteristic changes for the amide I and II bands of G5OH and APS-G5OH at different pH, respectively. As can be seen in more detail in Fig. 6, the amide I band of as-prepared G5OH shifts to a higher wavenumber with decreasing pH. Conversely, no significant shift was observed with increasing pH. It should be noted that the amide II band of as-prepared G5OH changes under neither acidic nor basic conditions. In contrast, the amide I band of as-prepared APS-G5OH shifts to a higher wavenumber with decreasing pH but drastically to a lower wavenumber with increasing pH. The amide II band of as-prepared APS-G5OH does not change further with decreasing pH but shifts to a lower wavenumber with increasing pH. The amide I band for both G5OH and APS-G5OH shifts to a higher wavenumber under acidic conditions, likely due to the enhancement in the strength of hydrogen bonding.

These results indicate that the pore surface of G5OH and APS-G5OH was significantly altered under different pH and can be manipulated on the basis of the following explanations. (i) The strength of the hydrogen bonding on the pore surface of PAMAM dendrimers is likely to be enhanced under acidic conditions [12]. (ii) The pK_a value of the tertiary amine of the pore surface is in the range between 3 and 6. Therefore, the tertiary amines of the pore surface of PAMAM dendrimers are protonated under acidic conditions, resulting in the formation of tertiary ammonium cations that makes more rigid-dendritic globular structure due to the strong charge-charge repulsions [13]. (iii) The anions of permonosulfuric acid and/or sulfuric acid, which are generated from the hydrolysis of APS, interacted with G5OH. Furthermore, the interaction of these anions with G5OH can change under different pH.

3.3. X-ray photoelectron spectra of as-prepared pristine and APS-G5OH dendrimer

The chemical states of C 1*s*, N 1*s*, O 1*s*, and S 2*p* of as-prepared G5OH and APS-G5OH films were examined by XPS measurements

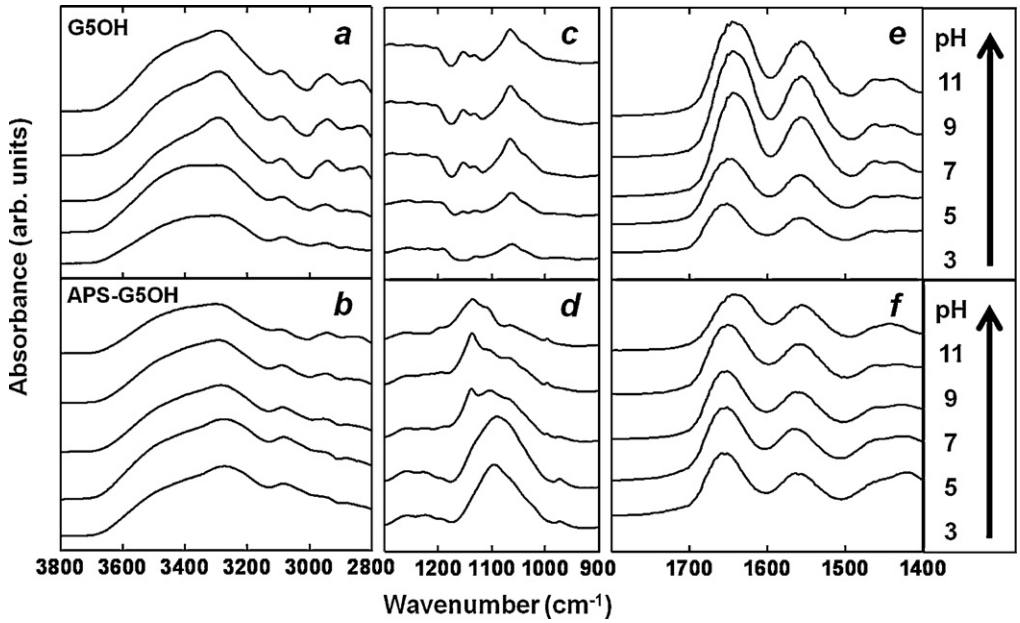

Fig. 5. FT-IR spectral profiles of G5OH and APS-G5OH films. The films were prepared from aqueous solutions of 0.2 mM G5OH and APS-G5OH solutions at different pH.

in order to rationalize the strong fluorescence behavior of APS-G5OH. XPS spectra in the C 1*s* region for G5OH and APS-G5OH films at any pH showed peaks at the same binding energy of 284.2 eV, indicating that the dendrimer films were free from a charging effect (Fig. S1) [19]. Fig. 7 shows the XPS spectra of as-prepared G5OH and APS-G5OH in the N 1*s* and O 1*s* regions. The binding energies of as-prepared G5OH and APS-G5OH are significantly different in the N 1*s* regions. The N 1*s* spectra of as-prepared G5OH can be deconvoluted into two component peaks centered at the binding energies of 399.4 and 400.1 eV for tertiary amine and amide groups, respectively [17b,20]. The binding energy of amide nitrogen retained the same position observed at (400.0 eV); however, the tertiary amine peak shifted largely to a deeper level (401.9 eV) due to the formation of a tertiary ammonium cation by protonation of the tertiary amine in the case of the as-prepared APS-G5OH PAMAM dendrimer (pH 5.2) [21]. It should be noted that the binding energy of O 1*s* of both as-prepared G5OH (532.1 eV) and APS-G5OH (532.2 eV) did not show any significant changes in the O 1*s* regions [17b,20].

3.3.1. X-ray photoelectron spectra of pristine and APS-G5OH dendrimers in the N 1s region under different pH

Fig. 8 shows the XPS profiles of G5OH and APS-G5OH films prepared from the sample solutions at pH 3 and 11 in the N 1*s* region to ensure the influence of pH on the dendritic structures. G5OH showed the binding energies of amide nitrogen and a tertiary ammonium cation peak centered at 400.1 and 402.3 eV in the N 1*s* region, respectively, at pH 3. No characteristic tertiary ammonium cation peak was observed for G5OH at pH 11; however, a weak peak was observed at 400.6 eV. In addition, no significant changes in the binding energy of amide nitrogen were observed at 400.0 eV at pH 11 (Fig. 8a). APS-G5OH also showed a similar trend in the N 1*s* region, similarly to G5OH at pH 3 and 11 (Fig. 8b, Table 1). It should be noted that the intensity of the tertiary ammonium cation peak of APS-G5OH is much stronger than that of pristine G5OH relative to the amide nitrogen peak at pH 3. In addition, the binding energy of as-prepared APS-G5OH (401.9 eV) shifts further to a higher binding energy, 402. 2 eV at pH 3, indicating that tertiary amine nitrogen was not fully protonated in the case of as-prepared APS-G5OH (pH 5.2). The unprotonated tertiary amine groups of as-prepared APS-G5OH were further protonated with decreasing pH, and, thus, the tertiary ammonium cation peak shifted further to a deeper level (ca. 0.3 eV) compared to as-prepared APS-G5OH. It is worthy of note that a weak peak with slightly higher binding energy than that of the tertiary amine was observed in the cases of both G5OH and APS-G5OH at 400.6 eV and 401.2 eV, respectively, at pH 11, indicating that the tertiary ammonium cation is deprotonated, but not completely, even at higher pH [22]. However, some more direct evidence should be needed to correlate the protonation and deprotonation of the tertiary amine at different pH. Neither G5OH nor APS-G5OH showed any characteristic changes in the O 1*s* region at either pH 3 or 11, as shown in the supporting information (Fig. S2, Table 1), indicating that the chemical state of oxygen of both amide and surface hydroxyl groups was not affected under either the acidic or the basic condition.

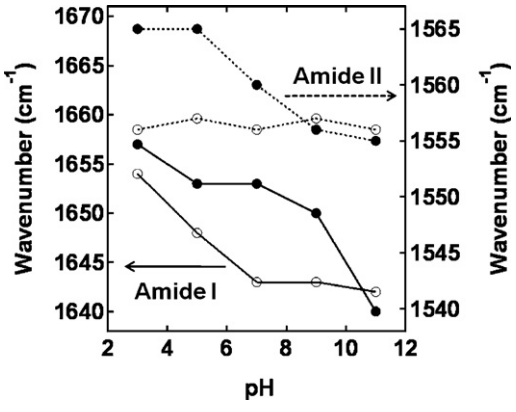

Fig. 6. pH dependences of amide I and II bands of G5OH (open circle) and APS-G5OH (closed circle).

3.3.2. X-ray photoelectron spectra of APS-G5OH dendrimer in the S 2p region under different pH

Fig. 9 shows the XPS profiles of as-prepared APS-G5OH and at pH 3 and 11 in the S 2*p* region. All profiles show two main peaks of S_A and S_B corresponding to the sulfur atoms, which are in the oxidation state of VI (e.g., SO_4^{2-}) and II (e.g., $S_2O_3^{2-}$, S^{2-}), respectively. The hydrolysis of APS would produce unstable free radicals ($SO_4^{\bullet-}$), hydrogen peroxide, and peroxymonosulfate, which are converted

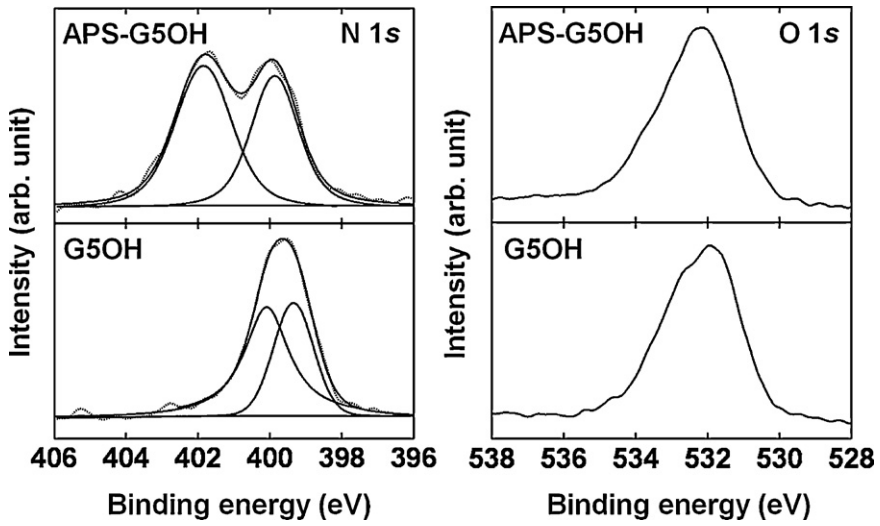

Fig. 7. XPS profiles for the as-prepared G5OH and APS-G5OH in the N 1*s* and O 1*s* regions.

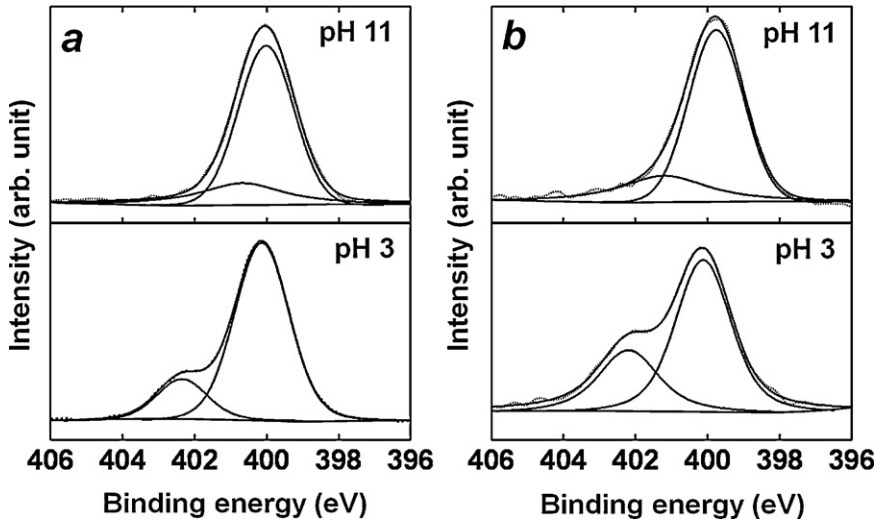

Fig. 8. XPS profiles for G5OH (a) and APS-G5OH (b) in the N 1*s* regions under acidic (pH 3) and basic (pH 11) conditions.

further into stable sulfur VI and II ions [9b]. It has been reported that the core-level S 2*p* peaks of H_2SO_4 also show similar S (VI) and S (II) peaks [23]. The S_A peak can be resolved into two component peaks of spin orbit doublets, S $2p_{3/2}$ and S $2p_{1/2}$. The spin orbit doublets of as-prepared APS-G5OH (S $2p_{3/2}$ = 168.6 eV and S $2p_{1/2}$ = 170.0 eV) shift to a shallower level under an acidic condition (pH 3) centered at 168.4 and 169.5 eV, respectively. On the other hand, the S $2p_{3/2}$ peak shifts to a deeper level (168.9 eV), but the S $2p_{1/2}$ peak retains the same value, similarly to as-prepared APS-G5OH (170.0 eV) at pH 11. The spin orbit splitting value of as-prepared APS-G5OH (1.40 eV) achieved a lower value at both pH 3 and 11 (1.10 eV). It should be noted that the doublet peak of S_B for as-prepared APS-G5OH showed only a slight change at pH 3; however, the intensity of the S_B peak becomes much stronger than that of S_A at pH 11. These results indicate that the oxidation state of both VI and II corresponding to sulfur atoms of APS-G5OH, as well as their interactions with G5OH, is significantly altered under different pH.

Table 1
XPS binding energy assignments of the core level peaks for as-prepared G5OH and APS-G5OH and under different pH.

Sample	N 1*s* (eV)		O 1*s* (eV)	S 2*p* (eV)		
	O=C–**N**H	–**N**<	(–C**O**, S**O**, $\mathbf{O}_2$, etc.)	**S** (VI)		**S** (II)
				2 $p_{1/2}$	2 $p_{3/2}$	
G5OH (as-prepared)	400.1	399.4	532.1	–	–	–
APS-G5OH (as-prepared)	400.0	401.9	532.2	170.0	168.6	163.6
G5OH (pH 3)	400.1	402.4	532.2	–	–	–
G5OH (pH 11)	400.0	400.6	532.2	–	–	–
APS-G5OH (pH 3)	400.1	402.2	532.1	169.5	168.4	163.6
APS-G5OH (pH 11)	399.9	401.2	532.1	170.0	168.9	163.6

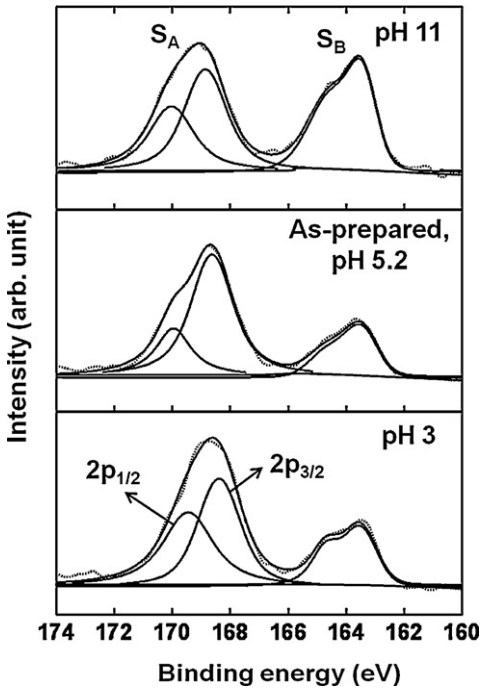

Fig. 9. XPS profiles for APS-treated G5 PAMAM dendrimers in the S 2*p* region under different pH.

Fig. 10 summarizes the change of the dendritic structure of pristine G5OH by APS treatment as well as the influence of pH on the dendritic structures of pristine G5OH and APS-G5OH. G5OH contains hydroxyl groups on its periphery as well as tertiary amines and amide functional groups on the pore surface. From the FT-IR and XPS results, the peripheral hydroxyl and amide nitrogen of the pore surface of G5OH are not affected by the APS treatment. However, the tertiary amine groups are protonated by APS treatment due to the falling of pH from 7.6 to 5.2, and, thus APS-G5OH fills with tertiary ammonium cations on the pore surface. The sulfur (VI and II) ions interact with these cations on the pore surface of APS-G5OH (Fig. 10b). The peripheral hydroxyl and amide nitrogen of both G5OH and APS-G5OH are not affected by the change in the pH. On the other hand, the tertiary amine groups of both G5OH and APS-G5OH are significantly affected by the change in the pH. The pH of the pristine G5OH is 7.2; therefore, G5OH is not protonated in an aqueous solution. Tertiary ammonium cations are formed by the protonation of the tertiary amine of G5OH, when the pH of the pristine G5OH solution is down to acidic condition. On the other hand, the tertiary ammonium cations of the pore surface of G5OH are deprotonated when the solution achieves a basic condition (Fig. 10c). A similar trend was observed in the case of APS-G5OH under acidic and basic conditions, similarly to the case of G5OH. The protonated tertiary amine groups of APS-G5OH due to the falling of pH by APS treatment which are deprotonated when the pH of the solution become to basic condition. The sulfur ions (VI and II) interact with APS-G5OH regardless of the change in the pH, as shown in Fig. 10d. Therefore, the enhancement in the fluorescence of APS-G5OH is most likely attributed the changes in the local environment of the branching units of the dendrimer molecules are summarized as follows. The formation of rigid, globular dendritic structures due to the strong charge–charge repulsions between tertiary ammonium cations [13] and the strong hydrogen bonding between –C=O and –N–H moieties in amide groups under acidic condition. Thus, the globular rigid-dendritic structure most likely exhibits strong fluorescence rather than vibrational relaxation [24].

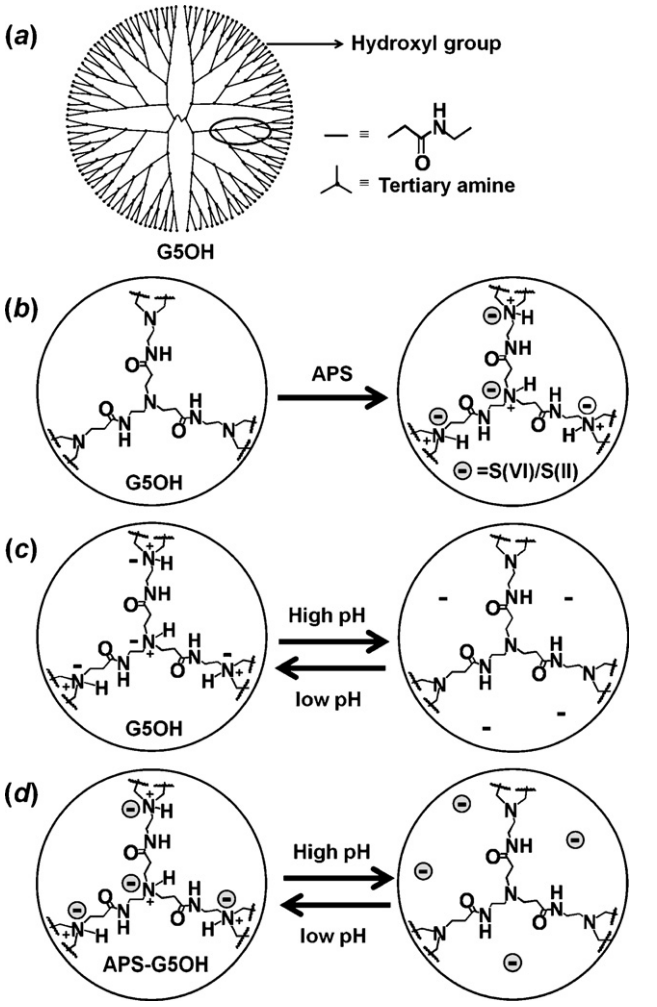

Fig. 10. (a) Structure of the ethylenediamine core G5OH dendrimer. The shaded area for the schematic illustration of the changes in the dendritic structures of G5OH dendrimer by APS treatment and at different pH is shown. (b) Schematic illustrations of the formation of APS-G5OH from G5OH by APS treatment. Schematic illustrations of pristine G5OH (c) and APS-G5OH (d) under acidic and basic conditions.

4. Conclusion

The dendritic structures of both pristine and APS-treated, hydroxyl-terminated, generation-five PAMAM dendrimers were examined at different pH. The pH of the APS-treated PAMAM dendrimer is 5.2, while that of the pristine PAMAM dendrimers is 7.6. No significant changes were observed for the peripheral hydroxyl or the amide nitrogen of PAMAM dendrimers by APS treatment. Tertiary ammonium cations were formed on the pore surface of the PAMAM dendrimer by protonation of tertiary amine groups during APS treatment as well as under acidic conditions; thus, the PAMAM dendrimer fills with tertiary ammonium cations (R_3NH^+, $R = CH_2^-$) on the pore surface. Neither the peripheral hydroxyls nor the amide nitrogen of both pristine and APS-treated PAMAM dendrimers were significantly affected at any pH. Therefore, the formation of tertiary ammonium cations on the pore surface of the APS-treated PAMAM dendrimer is most likely involved in the fluorescence enhancement, while the weakly fluorescent pristine PAMAM dendrimer possesses tertiary amine groups on the pore surface.

Acknowledgement

The authors thank Mr. Koji Funaba, Nanotechnology Innovation Center, National Institute for Materials Science for his help with spectroscopic studies.

Appendix A. Supplementary data

Supplementary data associated with this article can be found, in the online version, at doi:10.1016/j.jphotochem.2011.09.012.

References

[1] (a) G. Pistolis, A. Malliaris, C.M. Paleos, D. Tsiourvas, Study of poly(amidoamine) starburst dendrimers by fluorescence probing, Langmuir 13 (1997) 5870–5875;
(b) D.A. Wade, P.A. Torres, S.A. Tucker, Spectrochemical investigations in dendritic media: evaluation of nitromethane as a selective fluorescence quenching agent in aqueous carboxylate-terminated polyamido amine (PAMAM) dendrimers, Anal. Chim. Acta 397 (1999) 17–31;
(c) O. Varnavski, R.G. Ispasoiu, L. Balogh, D. Tomalia, T. Goodson III, Ultrafast time-resolved photoluminescence from novel metal–dendrimer nanocomposites, J. Chem. Phys. 114 (2001) 1962–1965;
(d) C.L. Larson, S.A. Tucker, Intrinsic fluorescence of carboxylate-terminated polyamido amine dendrimers, Appl. Spectrosc. 55 (2001) 679–683.

[2] (a) E.C. Wiener, S. Konda, A. Shadron, M. Brechbiel, O. Gansow, Targeting dendrimer-chelates to tumors and tumor cells expressing the high-affinity folate receptor, Invest. Radiol. 32 (1997) 748–754;
(b) J.F. Kukowska-Latallo, K.A. Candido, Z. Cao, S.S. Nigavekar, I.J. Majoros, T.P. Thomas, L.P. Balogh, M.K. Khan, J.R. Baker, Nanoparticle targeting of anticancer drug improves therapeutic response in animal model of human epithelial cancer, Cancer Res. 65 (2005) 5317–5324;
(c) I.J. Majoros, T.P. Thomas, C.B. Mehta, J.R. Baker, Poly(amidoamine) dendrimer-based multifunctional engineered nanodevice for cancer therapy, J. Med. Chem. 48 (2005) 5892–5899;
(d) I.J. Majoros, A. Myc, T. Thomas, C.B. Mehta, J.R. Baker, PAMAM dendrimer-based multifunctional conjugate for cancer therapy: synthesis, characterization, and functionality, Biomacromolecules 7 (2006) 572–579.

[3] S.H. Wang, X. Shi, M.V. Antwerp, Z. Cao, S.D. Swanson, X. Bi, J.R. Baker, Dendrimer-functionalized iron oxide nanoparticles for specific targeting and imaging of cancer cells, Adv. Funct. Mater. 17 (2007) 3043–3050.

[4] L. Albertazzi, B. Storti, L. Marchetti, F. Beltram, Delivery and subcellular targeting of dendrimer-based fluorescent pH sensors in living cells, J. Am. Chem. Soc. 132 (2010) 18158–18167.

[5] (a) M. Zhao, R.M. Crooks, Homogeneous hydrogenation catalysis with monodisperse, dendrimer-encapsulated Pd and Pt nanoparticles, Angew. Chem. Int. Ed. 38 (1999) 364–366;
(b) K. Esumi, A. Suzuki, A. Yamahira, K. Torigoe, Role of poly(amidoamine) dendrimers for preparing nanoparticles of gold, platinum, and silver, Langmuir 16 (2000) 2604–2608;
(c) R.M. Crooks, M. Zhao, L. Sun, V. Chechik, L.K. Yeung, Dendrimer-encapsulated metal nanoparticles: synthesis, characterization, and applications to catalysis, Acc. Chem. Res. 34 (2001) 181–190;
(d) O.S. Alexeev, A. Siani, G. Lafaye, C.T. Williams, H.J. Ploehn, M.D. Amiridis, EXAFS characterization of dendrimer-Pt nanocomposites used for the preparation of Pt/γ-Al_2O_3 catalysts, J. Phys. Chem. B 110 (2006) 24903–24914;
(e) N.N. Hoover, B.J. Auten, B.D. Chandler, Tuning supported catalyst reactivity with dendrimer-templated Pt-Cu nanoparticles, J. Phys. Chem. B 110 (2006) 8606–8612.

[6] J. Zheng, J.T. Petty, R.M. Dickson, High quantum yield blue emission from water-soluble Au_8 nanodots, J. Am. Chem. Soc. 125 (2003) 7780–7781.

[7] X.C. Wu, A.M. Bittner, K. Kern, Synthesis, photoluminescence, and adsorption of CdS/dendrimer nanocomposites, J. Phys. Chem. B 109 (2005) 230–239.

[8] W.I. Lee, Y. Bae, A.J. Bard, Strong blue photoluminescence and ECL from OH-terminated PAMAM dendrimers in the absence of gold nanoparticles, J. Am. Chem. Soc. 126 (2004) 8358–8359.

[9] (a) J.F. Gall, G.L. Church, R.L. Brown, Solubility of ammoniumpersulfate in water and in solutions of sulfuric acid and ammonium sulfate, J. Phys. Chem. 47 (1943) 645–649;
(b) M. Mazur, Preparation of three-dimensional polymeric structures using gas bubbles as templates, J. Phys. Chem. C 112 (2008) 13528–13534;
(c) A.A. Qaiser, M.M. Hyland, D.A. Patterson, Control of polyaniline deposition on microporous cellulose ester membranes by in situ chemical polymerization, J. Phys. Chem. B 113 (2009) 14986–14993.

[10] (a) D. Wang, T. Imae, Fluorescence emission from dendrimers and its pH dependence, J. Am. Chem. Soc. 126 (2004) 13204–13205;
(b) D. Wang, T. Imae, M. Miki, Fluorescence emission from PAMAM and PPI dendrimers, J. Colloid Interface Sci. 306 (2007) 222–227.

[11] (a) A. Pevsner, M. Diem, Infrared spectroscopic studies of major cellular components. Part I: the effect of hydration on the spectra of proteins, Appl. Spectrosc. 55 (2001) 788–793;
(b) D.S. Deutsch, A. Siani, P.T. Fanson, H. Hirata, S. Matsumoto, C.T. Williams, M.D. Amiridis, FT-IR investigation of the thermal decomposition of poly(amidoamine) dendrimers and dendrimer–metal nanocomposites supported on Al_2O_3 and ZrO_2, J. Phys. Chem. C 111 (2007) 4246–4255.

[12] D.I. Malyarenko, R.L. Vold, G.L. Hoatson, Solid state deuteron NMR studies of polyamidoamine dendrimer salts. 1. Structure and hydrogen bonding, Macromolecules 33 (2000) 1268–1279.

[13] (a) W. Chen, D.A. Tomalia, J.L. Thomas, Unusual pH-dependent polarity changes in PAMAM dendrimers: evidence for pH-responsive conformational changes, Macromolecules 33 (2000) 9169–9172;
(b) M.H. Kleinman, J.H. Flory, D.A. Tomalia, N.J. Turro, Effect of protonation and PAMAM dendrimer size on the complexation and dynamic mobility of 2-naphthol, J. Phys. Chem. B 104 (2000) 11472–11479;
(c) K. Funayama, T. Imae, K. Aoi, K. Tsutsumiuchi, M. Okada, M. Furusaka, M. Nagao, Small-angle neutron scattering investigations of layer-block dendrimers in aqueous solutions, J. Phys. Chem. B 107 (2003) 1532–1539.

[14] (a) R.A. Nyquist, C.L. Putzig, M.A. Leugers, Handbook of Infrared and Raman Spectra of Inorganic Compounds and Organic Salts, Academic Press, San Diego, CA, 1997;
(b) H. Siebner-Freibach, Y. Hadar, S. Yariv, I. Lapides, Y. Chen, Thermospectroscopic study of the adsorption mechanism of the hydroxamic siderophore ferrioxamine B by calcium montmorillonite, J. Agric. Food Chem. 54 (2006) 1399–1408;
(c) M. Kumar, S. Singh, V.K. Shahi, Cross-linked poly(vinyl alcohol)-poly(acrylonitrile-*co*-2-dimethylamino ethylmethacrylate) based anion-exchange membranes in aqueous media, J. Phys. Chem. B 114 (2010) 198–206.

[15] (a) D. Lin-Vien, N.B. Colthup, W.G. Fateley, J.G. Grasselli, The Handbook of Infrared and Raman Characteristic Frequencies of Organic Molecules, Academic Press, San Diego, CA, 1991;
(b) R.M. Silverstein, G.C. Bassler, T.C. Morrill, Spectroscopic Identification of Organic Compounds, third ed., John Wiley and Sons, New York, 1991.

[16] E.D. Guldan, L.R. Schindler, J.T. Roberts, Growth and characterization of sulfuric acid under ultrahigh vacuum, J. Phys. Chem. 99 (1995) 16059–16066.

[17] (a) D. Liu, J. Gao, C.J. Murphy, C.T. Williams, In situ attenuated total reflection infrared spectroscopy of dendrimer-stabilized platinum nanoparticles adsorbed on alumina, J. Phys. Chem. B 108 (2004) 12911–12916;
(b) O. Ozturk, T.J. Black, K. Perrine, K. Pizzolato, C.T. Williams, F.W. Parsons, J.S. Ratliff, J. Gao, C.J. Murphy, H. Xie, H.J. Ploehn, D.A. Chen, Thermal decomposition of generation-4 polyamidoamine dendrimer films: decomposition catalyzed by dendrimer-encapsulated Pt particles, Langmuir 21 (2005) 3998–4006.

[18] (a) A. Manna, T. Imae, K. Aoi, M. Okada, T. Yogo, Synthesis of dendrimer-passivated noble metal nanoparticles in a polar medium: comparison of size between silver and gold particles, Chem. Mater. 13 (2001) 1674–1681;
(b) G. Socrates, Infrared and Raman Characteristic Group Frequencies, Third ed., Wiley, Chichester, 2001.

[19] G. Saravanan, H. Abe, Y. Xu, N. Sekido, H. Hirata, S. Matsumoto, H. Yoshikawa, Y. Yamabe-Mitarai, Pt_3Ti nanoparticles: fine dispersion on SiO_2 supports, enhanced catalytic CO oxidation, and chemical stability at elevated temperatures, Langmuir 26 (2010) 11446–11451.

[20] (a) J. Charlier, V. Detalle, F. Valin, C. Bureau, G. Lécayon, Study of ultrathin polyamide-6,6 films on clean copper and platinum, J. Vac. Sci. Technol. A 15 (1997) 353–364;
(b) A.J. Wagner, G.M. Wolfe, D.H. Fairbrother, Reactivity of vapor-deposited metal atoms with nitrogen-containing polymers and organic surfaces studied by in situ XPS, Appl. Surf. Sci. 219 (2003) 317–328.

[21] (a) A. Adenier, M.M. Chehimi, I. Gallardo, J. Pinson, N. Vilà, Electrochemical oxidation of aliphatic amines and their attachment to carbon and metal surfaces, Langmuir 20 (2004) 8243–8253;
(b) G. Zhai, W.H. Yu, E.T. Kang, K.G. Neoh, C.C. Huang, D.J. Liaw, Functionalization of hydrogen-terminated silicon with polybetaine brushes via surface-initiated reversible addition-fragmentation chain-transfer (RAFT) polymerization, Ind. Eng. Chem. Res. 43 (2004) 1673–1680;
(c) M. Datta, H.J. Mathieu, D. Landolt, Characterization of transpassive films on nickel by sputter profiling and angle resolved AES/XPS, Appl. Surf. Sci. 18 (1984) 299–314.

[22] M.S. Diallo, K. Falconer, J.H. Johnson Jr., W.A. Goddard III, Dendritic anion hosts: perchlorate uptake by G5-NH_2 poly(propyleneimine) dendrimer in water and model electrolyte solutions, Environ. Sci. Technol. 41 (2007) 6521–6527.

[23] R. Graupner, J. Abraham, A. Vencelová, T. Seyller, F. Hennrich, M.M. Kappes, A. Hirsch, L. Ley, Doping of single-walled carbon nanotube bundles by Bronsted acids, Phys. Chem. Chem. Phys. 5 (2003) 5472–5476.

[24] (a) B. Valeur, Molecular Fluorescence: Principles and Applications, Wiley-VCH, Verlag GmbH, Weinheim, Germany, 2001;
(b) Y. Lin, J.-W. Gao, H.-W. Liu, Y.-S. Li, Synthesis and characterization of hyperbranched poly(ether amide)s with thermoresponsive property and unexpected strong blue photoluminescence, Macromolecules 42 (2009) 3237–3246.